Output summary of the CUED program

The CUED program is developed and maintained by:

Chair of Computational Condensed Matter Theory
Institute of Theoretical Physics
University of Regensburg
Universitätsstraße 31
D - 93053 Regensburg
Germany

Date of execution: October 25, 2021
Run time: 32.2 s
Number of used processors: 2

Contact:

Jan Wilhelm
Ferdinand Evers

Contributors (in alphabetic order):

Jack Crewse
Patrick Grössing
Adrian Seith

Contents

1 How to cite and reference CUED

When using the CUED software package, please reference to CUED by citing the following publication:

[1] J. Wilhelm, P. Grössing, A. Seith, J. Crewse, M. Nitsch, L. Weigl, C. Schmid, and F. Evers, *Semiconductor-Bloch Formalism: Derivation and Application to High-Harmonic Generation from Dirac Fermions*, Phys. Rev. B **103**, 125419 (2021).

2 Electric-field pulse

The following electric driving field is employed in the simulation:

$$\mathbf{E}(t) = E(t)\,\hat{e}_\phi\,, \qquad E(t) = E_0\,\sin\Big(2\pi f_0\,(1 + f_{\text{chirp}}t)\,t + \varphi\Big)\,e^{-t^2/\sigma^2}\,. \tag{1}$$

The pulse is sketched in Fig. 1. The following parameters are used in the simulation:

- Amplitude: $E_0 = 10.0\,\text{MV/cm}$

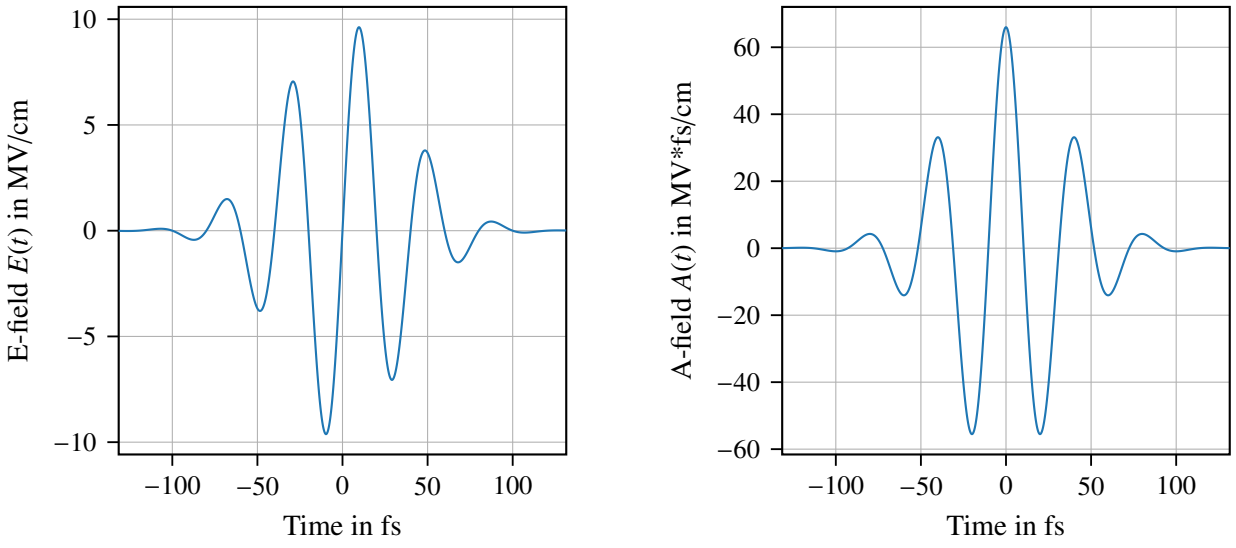

Figure 1: Left: Electric driving field $E(t)$, right: Gauge field $A(t)$ from Eq. (2).

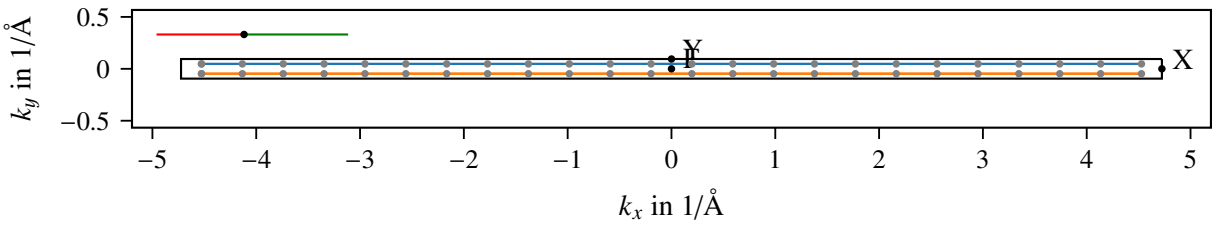

Figure 2: Brillouin zone (BZ) and 24×2 k-point mesh. The BZ is indicated by the black rectangle. Gray points indicate k-points, colored lines indicate k-points that are coupled via the term $\mathbf{E}(t) \cdot \nabla_{\mathbf{k}}$. The green and red line at the top left corner sketch $\mathbf{A}_{\text{max}} \coloneqq \hat{e}_\phi \max(-qA(t)/\hbar)$ and $\mathbf{A}_{\text{min}} \coloneqq \hat{e}_\phi \min(-qA(t)/\hbar)$ indicating the extremal excursion of electrons in the BZ.

- $\hat{e}_\phi = \hat{e}_x$
- Pulse frequency: $f_0 = 25.0\,\text{THz}$
- Chirp: $f_{\text{chirp}} = 0.0\,\text{THz}$
- Carrier-envelope phase: $\phi = 0.0$
- $\sigma = 50.0\,\text{fs}$, full width at half maximum (FWHM) of the Gaussian envelope = 83.255 fs

The gauge field $\mathbf{A}(t) = A(t)\,\hat{e}_\phi$ follows from $\dot{\mathbf{A}}(t) = -\mathbf{E}(t)$. We compute $A(t)$ for the sketch in Fig. 1 as

$$\dot{A}(t) = -E(t) \qquad \Rightarrow \qquad A(t) = -\int_{-\infty}^{t} E(t')\,dt' \,. \tag{2}$$

3 Brillouin zone and *k*-point grid

A rectangle as Brillouin zone (BZ) with a mesh size of 30×2 is used. The BZ and a 24×2 k-point mesh is sketched in Fig. 2. Please note that in the params.py file, the BZ size (in case of a rectangular BZ) and the lattice parameter a (in case of a hexagonal BZ) are both given in atomic units, while the output here is in 1/Å (note: 1 atomic length unit = $1a_0 = 0.529$ Å, a_0: Bohr radius, 1 atomic inverse length unit = 1/(0.529 Å) = $1.890\,\text{Å}^{-1}$).

4 Hamiltonian, bandstructure and dipoles

The n-band Hamiltonian $h(\mathbf{k})$ is an $n \times n$ matrix that is given as an input. Diagonalizing $h(\mathbf{k})$ yields the band structure and the eigenvectors $|u_{n\mathbf{k}}\rangle$,

$$h(\mathbf{k})\,|u_{n\mathbf{k}}\rangle = \epsilon_n(\mathbf{k})\,|u_{n\mathbf{k}}\rangle\,. \tag{3}$$

Dipoles are computed from

$$\mathbf{d}_{nn'}(\mathbf{k}) = iq\,\langle u_{n\mathbf{k}}|\,\partial_{\mathbf{k}}\,|u_{n'\mathbf{k}}\rangle\,, \tag{4}$$

where $q = -e$ is the electron charge. The band structure and the dipoles are sketched in Fig. 3 and 4.

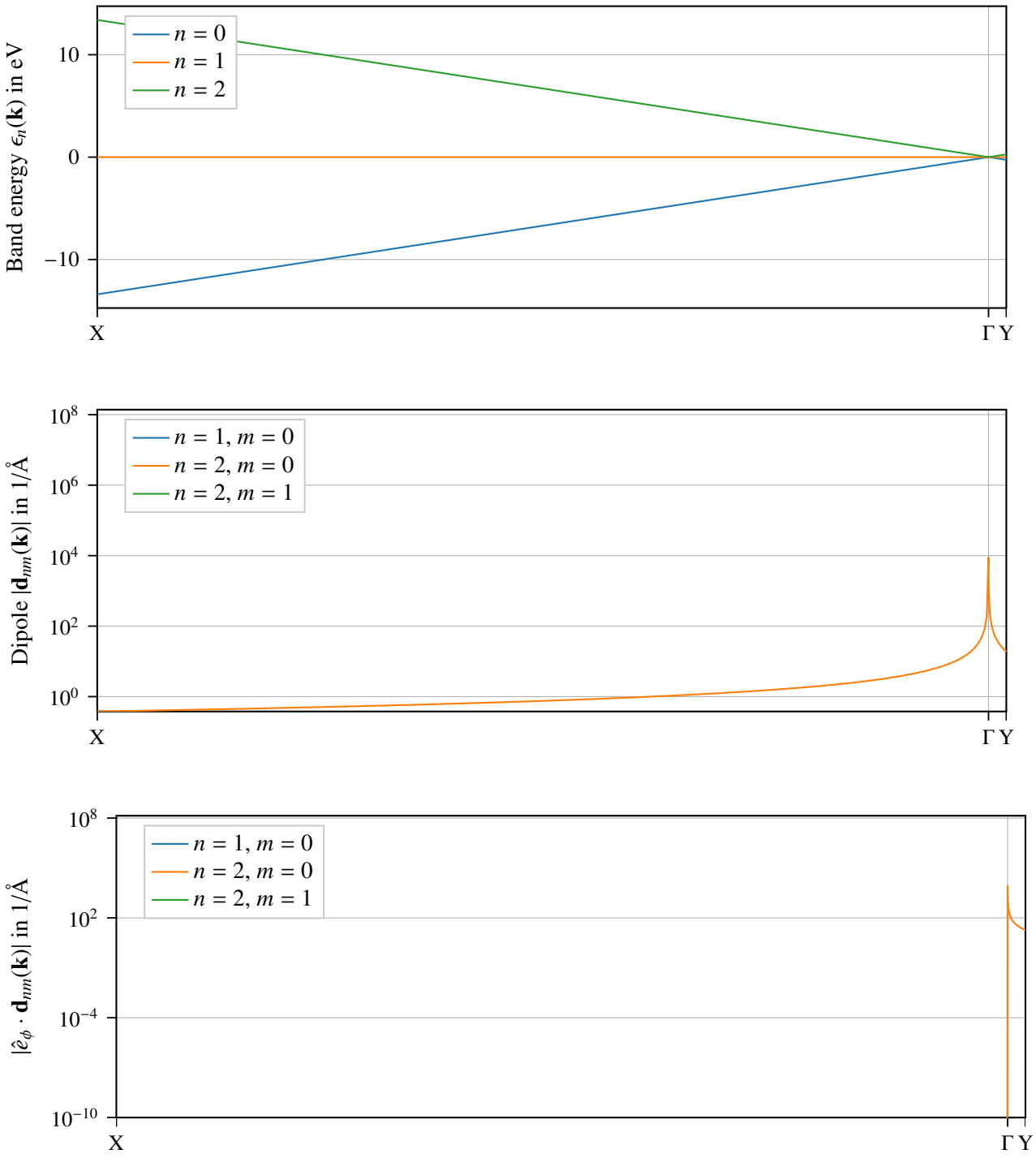

Figure 3: Top: Band structure $\epsilon_n(\mathbf{k})$ as computed from the Hamiltonian $h(\mathbf{k})$, see Eq. (3). Middle and bottom: Absolute value of the dipoles and projection of the dipole onto the axis of the electric field [this projection enters the semiconductor Bloch equations, Eq. (5)]. Dipoles below 10^{-10} Å are not displayed.

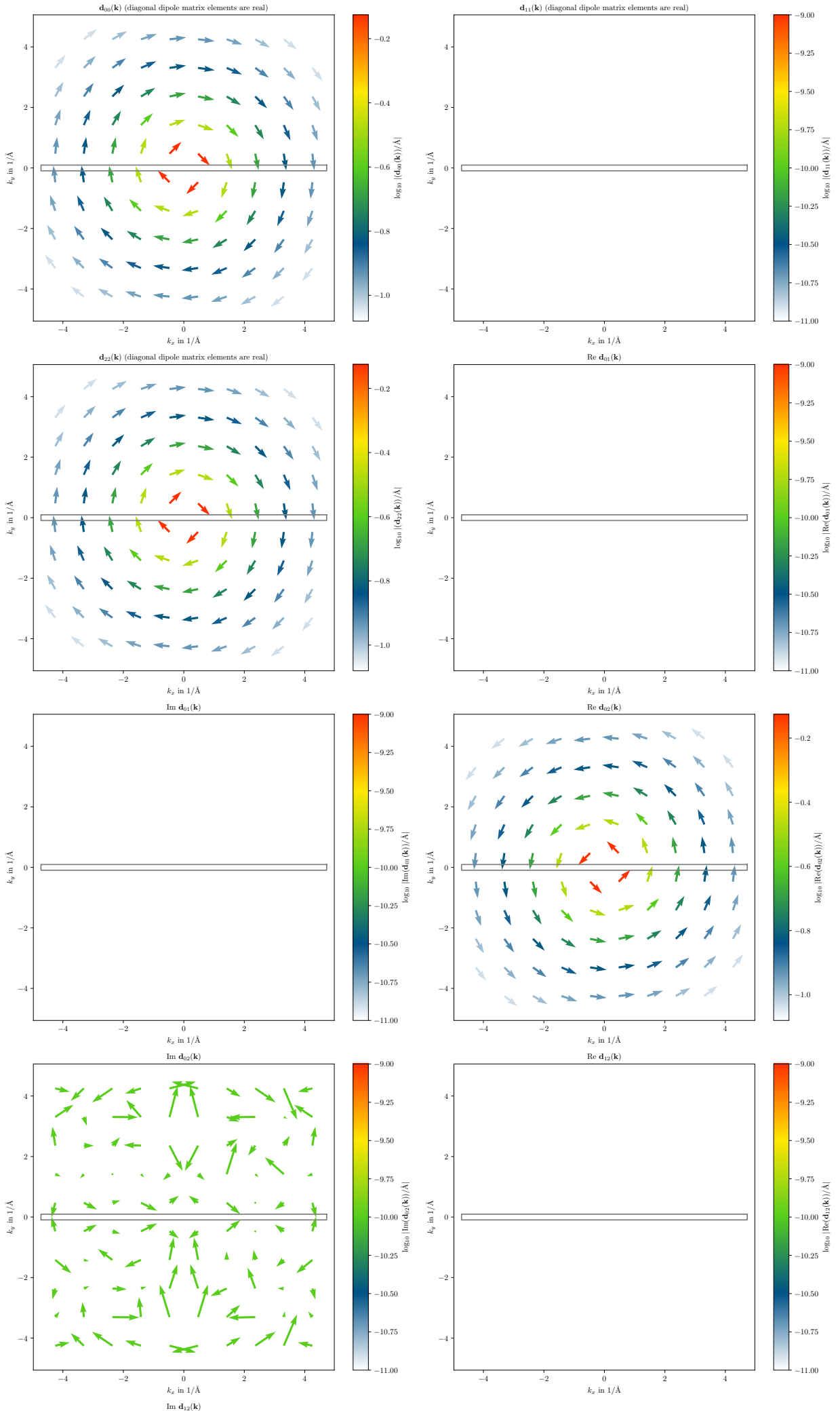
$\mathbf{d}_{00}(\mathbf{k})$ (diagonal dipole matrix elements are real)
$\mathbf{d}_{11}(\mathbf{k})$ (diagonal dipole matrix elements are real)
$\mathbf{d}_{22}(\mathbf{k})$ (diagonal dipole matrix elements are real)
Re $\mathbf{d}_{01}(\mathbf{k})$
Im $\mathbf{d}_{01}(\mathbf{k})$
Re $\mathbf{d}_{02}(\mathbf{k})$
Im $\mathbf{d}_{02}(\mathbf{k})$
Re $\mathbf{d}_{12}(\mathbf{k})$
Im $\mathbf{d}_{12}(\mathbf{k})$
k_x in 1/Å
k_y in 1/Å
$\log_{10}[|\mathbf{d}_{00}(\mathbf{k})|/\text{Å}]$
$\log_{10}[|\mathbf{d}_{11}(\mathbf{k})|/\text{Å}]$
$\log_{10}[|\mathbf{d}_{22}(\mathbf{k})|/\text{Å}]$
$\log_{10}[|\text{Re}(\mathbf{d}_{01}(\mathbf{k}))|/\text{Å}]$
$\log_{10}[|\text{Im}(\mathbf{d}_{01}(\mathbf{k}))|/\text{Å}]$
$\log_{10}[|\text{Re}(\mathbf{d}_{02}(\mathbf{k}))|/\text{Å}]$
$\log_{10}[|\text{Im}(\mathbf{d}_{02}(\mathbf{k}))|/\text{Å}]$
$\log_{10}[|\text{Re}(\mathbf{d}_{12}(\mathbf{k}))|/\text{Å}]$

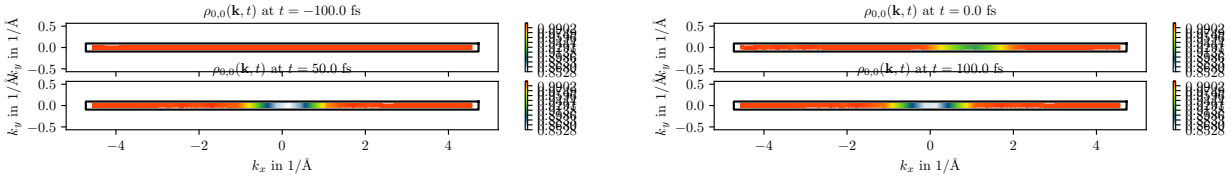

Figure 5: Time evolution of the 0-0 diagonal entry of the density matrix.

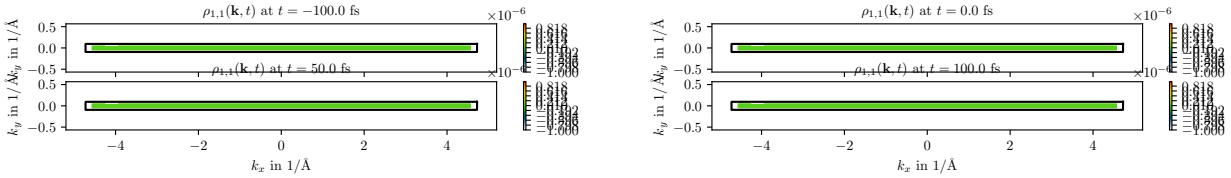

Figure 6: Time evolution of the 1-1 diagonal entry of the density matrix.

5 Time evolution of the density matrix

In case you choose the length gauge (`gauge = 'length'`, that is also the default) and $1/T_1 = 0$, we solve semiconductor Bloch equations in the length gauge, Eq. (50) in Ref. [1]:

$$\left[\frac{\partial}{\partial t} + q\mathbf{E}(t)\frac{\partial}{\partial \mathbf{k}}\right]\rho_{nn'}(\mathbf{k},t) = \left[i(\epsilon_{n'}(\mathbf{k}) - \epsilon_n(\mathbf{k})) - \frac{1-\delta_{nn'}}{T_2}\right]\rho_{nn'}(\mathbf{k},t) - i\mathbf{E}(t)\sum_{\underline{n}}\left(\rho_{n\underline{n}}(\mathbf{k};t)\mathbf{d}_{\underline{n}n'}(\mathbf{k}) - \mathbf{d}_{n\underline{n}}(\mathbf{k})\rho_{\underline{n}n'}(\mathbf{k};t)\right) \tag{5}$$

with a dephasing time $T_2 = 1$ fs. The time evolution of the density matrix is visualized in Figs. 5 – 9.

6 Time-dependent current

In case you choose the length gauge (`gauge = 'length'`, that is also the default), the current is computed from Eq. (67) in Ref. [1] as

$$\mathbf{j}(t) = q\sum_{nn'}\int_{\mathrm{BZ}}\frac{d\mathbf{k}}{(2\pi)^2}\,\langle u_{n\mathbf{k}}|\frac{\partial h(\mathbf{k})}{\partial \mathbf{k}}|u_{n'\mathbf{k}}\rangle\,\rho_{n'n}(\mathbf{k},t)\;. \tag{6}$$

The matrix element $\langle u_{n\mathbf{k}}|(\partial_{\mathbf{k}}h(\mathbf{k}))|u_{n'\mathbf{k}}\rangle$ can be computed from Eq. (68) in Ref. [1] as

$$\langle u_{n\mathbf{k}}|\frac{\partial h(\mathbf{k})}{\partial \mathbf{k}}|u_{n'\mathbf{k}}\rangle = \delta_{nn'}\partial_{\mathbf{k}}\epsilon_n(\mathbf{k}) + \frac{i}{q}\,\mathbf{d}_{nn'}(\mathbf{k})\,(\epsilon_n(\mathbf{k}) - \epsilon_{n'}(\mathbf{k}))\;. \tag{7}$$

In our case, the current is a two-dimensional vector. For generating meaningful plots, we project the current onto the axis $\hat{e}_\phi$ of the incoming E-field and its orthogonal direction $\hat{e}_{\phi+\pi/2}$:

$$j_\parallel(t) = \hat{e}_\phi\,\mathbf{j}(t)\;,\qquad j_\perp(t) = \hat{e}_{\phi+\pi/2}\,\mathbf{j}(t)\;, \tag{8}$$

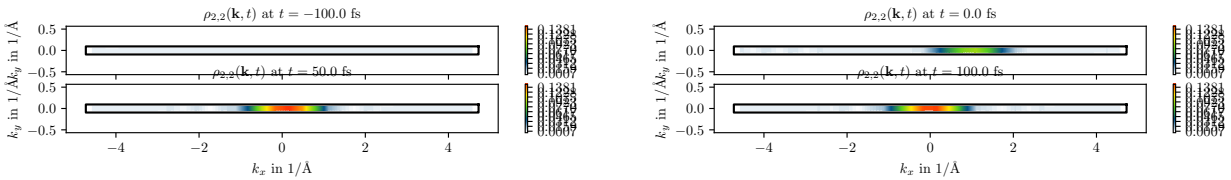

Figure 7: Time evolution of the 2-2 diagonal entry of the density matrix.

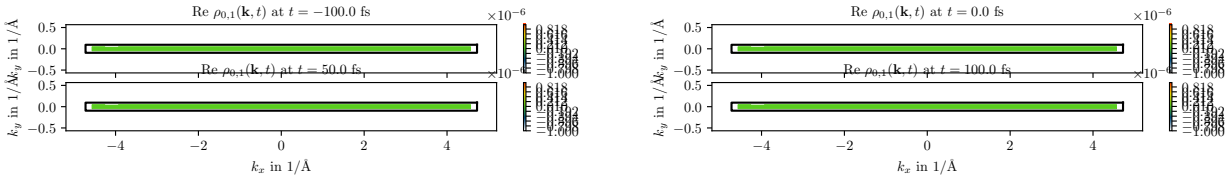

Figure 8: Time evolution of the real part of the 0-1 offdiagonal entry of the density matrix.

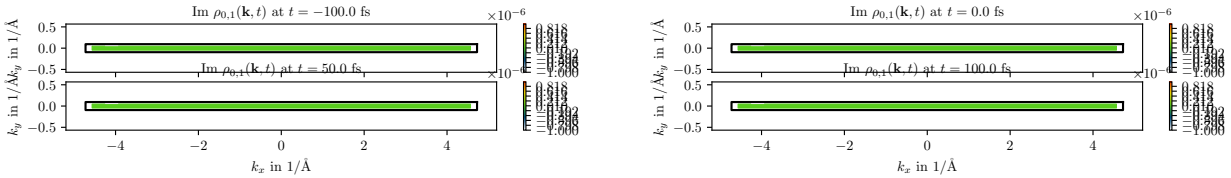

Figure 9: Time evolution of the imaginary part of the 0-1 offdiagonal entry of the density matrix.

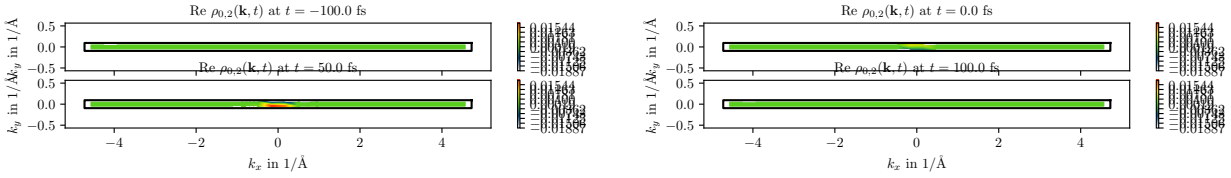

Figure 10: Time evolution of the real part of the 0-2 offdiagonal entry of the density matrix.

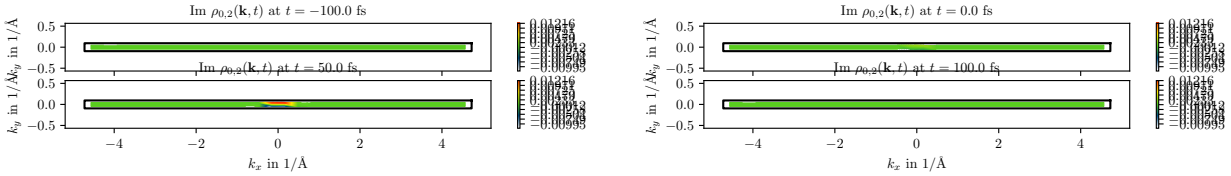

Figure 11: Time evolution of the imaginary part of the 0-2 offdiagonal entry of the density matrix.

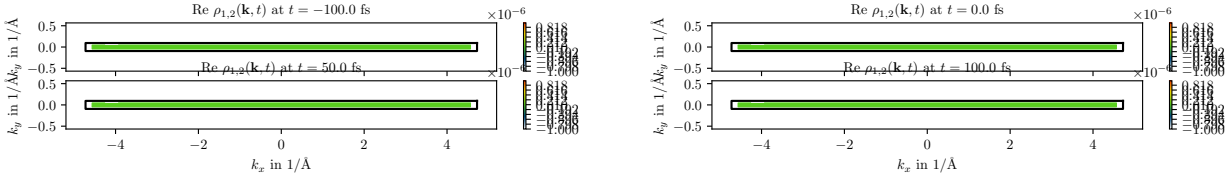

Figure 12: Time evolution of the real part of the 1-2 offdiagonal entry of the density matrix.

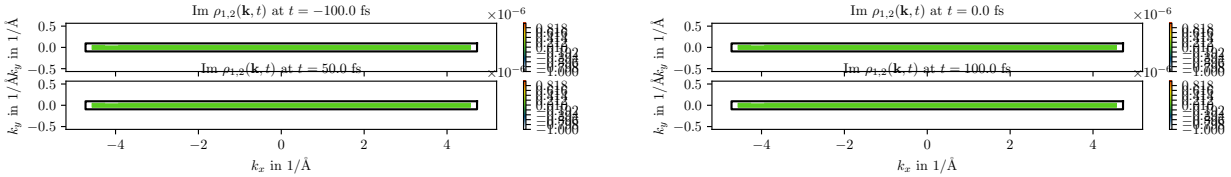

Figure 13: Time evolution of the imaginary part of the 1-2 offdiagonal entry of the density matrix.

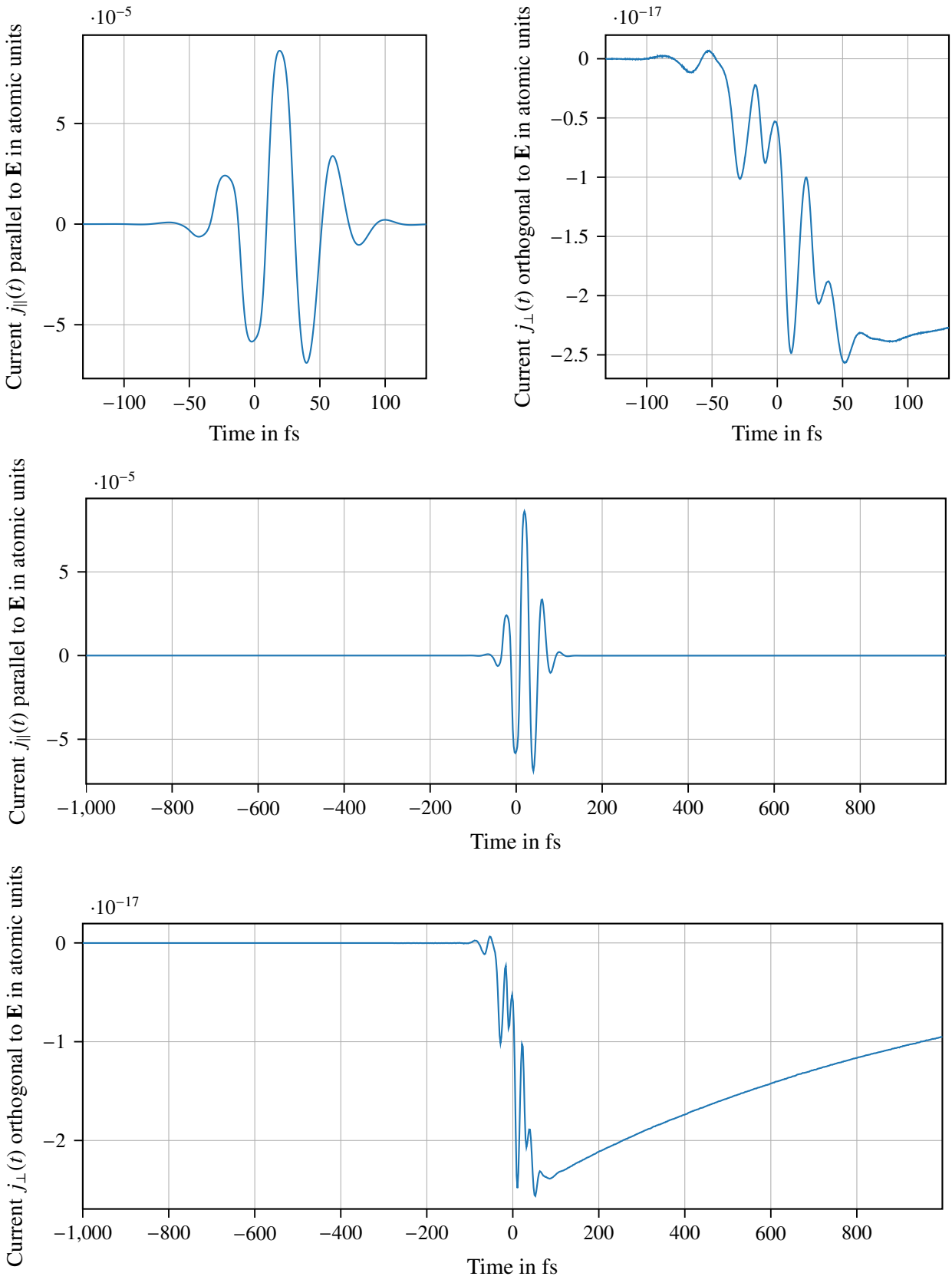

Figure 14: Components of the time-dependent current $\mathbf{j}(t)$: top left: parallel to the driving field, top right: orthogonal to the driving field, see Eq. (8). Middle and bottom: Current over the whole time window of the simulation.

and we recover

$$\mathbf{j}(t) = \hat{e}_\phi \, j_\parallel(t) + \hat{e}_{\phi+\pi/2} \, j_\perp(t) \, . \tag{9}$$

The time-dependent current is shown in Fig. 14.

7 Frequency-resolved emission spectrum

Experiments measure the frequency resolved emission intensity I, which is computed by Eq. (53) in Ref. [1]

$$I(\omega) = \frac{\omega^2}{3c^3} |\mathbf{j}(\omega)|^2 \, , \tag{10}$$

where c is the speed of light and $\mathbf{j}(\omega)$ is the Fourier transform of the current $\mathbf{j}(t)$. Since the current $\mathbf{j}(t)$ is not periodic in time, short-time Fourier transform (STFT) is used with a window function $w(t)$,

$$\mathbf{j}(\omega) = \frac{1}{\sqrt{2\pi}} \int_{-t_0}^{t_0} w(t) \, \mathbf{j}(t) \, e^{-i\omega t} \, . \tag{11}$$

As window, a Hann, Parzen and Gaussian window are available in the code. The emission is sketched in Fig. 15. When inserting Eq. (9) in the frequency domain, we have

$$I(\omega) = \frac{\omega^2}{3c^3} \left(|\mathbf{j}_\parallel(\omega)|^2 + |\mathbf{j}_\perp(\omega)|^2 \right) , \tag{12}$$

that motivates the definitions

$$I_\parallel(\omega) = \frac{\omega^2}{3c^3} |\mathbf{j}_\parallel(\omega)|^2 \, , \qquad I_\perp(\omega) = \frac{\omega^2}{3c^3} |\mathbf{j}_\perp(\omega)|^2 \, . \tag{13}$$

We recover $I(\omega) = I_\parallel(\omega) + I_\perp(\omega)$. The emission intensity of parallel and orthogonal polarized light is sketched in Fig. 15.

8 How to cite and reference CUED

When using the CUED software package, please reference to CUED by citing the following publication:

[1] J. Wilhelm, P. Grössing, A. Seith, J. Crewse, M. Nitsch, L. Weigl, C. Schmid, and F. Evers, *Semiconductor-Bloch Formalism: Derivation and Application to High-Harmonic Generation from Dirac Fermions*, Phys. Rev. B **103**, 125419 (2021).

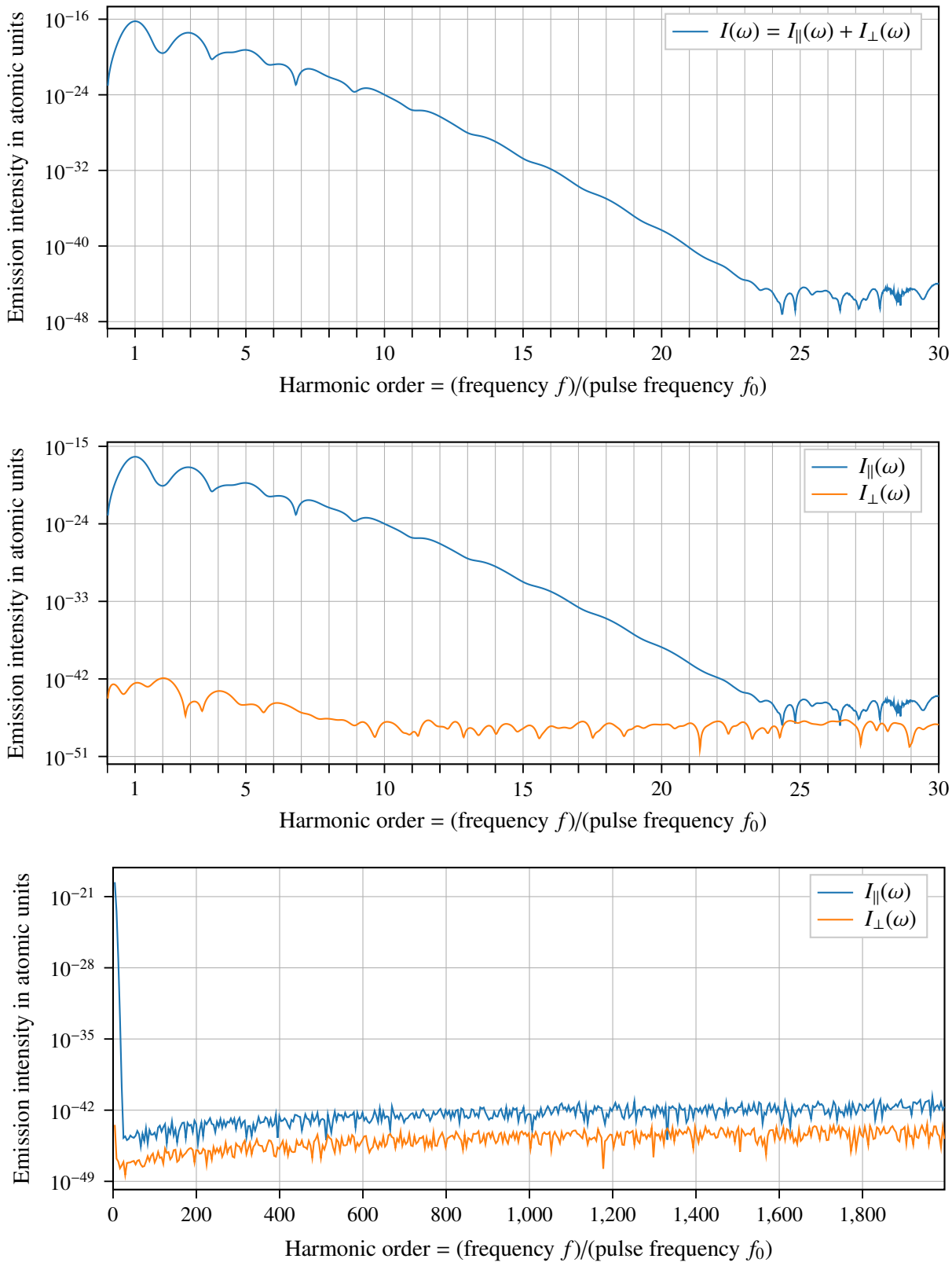

Figure 15: Top: Total emission intensity from the irradiated material computed from Eq. (10). Middle and bottom: Emission intensity of the polarization parallel and orthogonal to the incoming electric field from the irradiated material computed from Eq. (13). The data is displayed using two different frequency scales. The frequency is given by $f = \omega/(2\pi)$.